PROCEEDINGS OF SCIENCE

# Long-range dihadron correlations in high multiplicity pp and PbPb with CMS

**Sandra S. Padula*** **(for the CMS Collaboration)**
*Instituto de Física Teórica - UNESP, São Paulo, SP, Brazil*
*E-mail:* padula@ift.unesp.br

Charged dihadron angular correlations measured using the CMS detector at the LHC for both pp collisions at 7 TeV and PbPb collisions at 2.76 TeV are presented. New results on the ridge correlation structure in high multiplicity pp collisions are shown, where the event multiplicity, transverse momentum and pseudorapidity gap dependence of the ridge effect is investigated using the full statistics data collected in 2010. Both short- and long-range dihadron correlations are also studied in PbPb collision at a nucleon-nucleon center-of-mass energy of 2.76 TeV. The dependence of the jet- and ridge-region shape and yield on transverse momentum and collision centrality is discussed.

*The Seventh Workshop on Particle Correlations and Femtoscopy*
*September 20 - 24 2011*
*University of Tokyo, Japan*

*Speaker.

 

PoS(WPCF2011)023

Measurements of dihadron correlations have been giving insight into the properties of the dense Quantum Chromodynamic (QCD) medium formed in high energy heavy ion collisions for almost a decade. Particularly interesting was a more recent observation of pronounced dihadron correlations between particles with small relative azimuthal angles ($|\Delta\phi| \approx 0$) extending over a large relative pseudorapidity interval ($|\Delta\eta|$, where $\eta = -\ln[\tan(\theta/2)]$ and $\theta$ is the polar angle relative to the counterclockwise beam axis), as first measured in AuAu collisions at the Relativistic Heavy Ion Collider (RHIC)[1, 2].

At the Large Hadron Collider (LHC) those early measurements were extended into much higher beam energies as compared to those at RHIC [3, 4, 5, 6, 7]. Strikingly, such results in the new era started with high multiplicity events produced in pp collisions at $\sqrt{s} = 7$ TeV at the Compact Muon Solenoid (CMS) experiment, revealing also in this case a long (ridge-like) dihadron correlation in $|\Delta\eta|$ for pairs close in azimuthal angle [3]. The confirmation of the ridge-like structure in heavy ion experiments came afterwards, with its observation in the $0-5\%$ most central PbPb collisions at $\sqrt{s_{NN}} = 2.76$ TeV [4, 5]. More recently, those results were expanded in CMS for all collision centralities and over a broader range of hadron traverse momentum $p_T$, as can be seen in Ref. [6, 7].

The CMS detector has nearly $4\pi$ solid angle acceptance and is particularly suited for the study of dihadron correlations. Such measurement is based primarily on data from the inner tracker, consisting of silicon pixel and strip detectors, contained within the 3.8 T axial magnetic field of the large superconducting solenoid. For PbPb collisions, the primary minimum-bias trigger uses signals from either the beam scintillator counters (BSC, $3.23 < |\eta| < 4.65$ ) or the steel/quartz-fibre Cherenkov forward hadron calorimeters (HF, $2.9 < |\eta| < 5.2$). Coincident signals from detectors located at both ends (i.e., a pair of BSC or a pair of HF modules) are required. A complete description of the CMS detector can be found in Ref. [8].

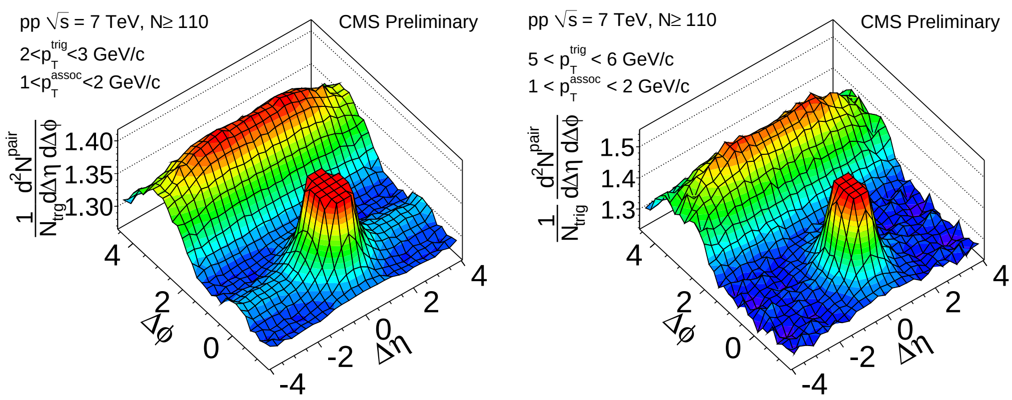


**Figure 1:** The long-range near-side dihadron correlation observed in high multiplicity ($N \geq 110$) pp collisions at 7 TeV is shown on the left; on the right, the ridge-like structure nearly disappears for higher $p_T^{trig}$ [6]. The jet peak around ($\Delta\eta \approx 0, \Delta\phi \approx 0$) is truncated for better displaying the surrounding structure.

Details of the analysis technique used for studying dihadron correlations are described in [3, 4, 6, 7]. This technique involves pairing a leading (*trigger*) hadron of one event with another hadron (*associate*) in the same event, either within the same or in different $p_T$ ranges. The background to such signal combination is formed by similarly pairing particles from mixed events. The ratio of the two is normalized by the pairs in the smallest bins around the zero interval in $|\Delta\phi|$ and $|\Delta\eta|$.

New analysis on the ridge correlation structure in high multiplicity pp collisions is performed to study the detailed event multiplicity, transverse momentum and $\Delta\eta$ dependence using the full statistics data collected in 2010 [6]. With a dedicated high multiplicity tracking high-level trigger (HLT) setup, the CMS experiment has a unique capability for studying this effect. The same analysis procedure as used in the ridge measurement of the central heavy-ion collisions is applied in order to make direct comparison to the heavy-ion results. The pp data used in this extended analysis are collected under almost the same condition as those used in the publication of the first pp ridge observation [3] with about a factor of 2 increase in statistics. In both the cases of high multiplicity pp and of PbPb events, the extracted 2D associated yield distributions in $(\Delta\eta, \Delta\phi)$ show a variety of characteristic features that are not present in minimum bias pp interactions.

The 2D per-trigger-particle associated yield distribution of charged hadrons as a function of $\Delta\eta$ and $\Delta\phi$ in high multiplicity ($N > 110$) pp collisions at $\sqrt{s} = 7$ TeV, considering trigger particles with $2 < p_T^{trig} < 3$ GeV/c and associated particles with $1 < p_T^{assoc} < 2$ GeV/c, is shown in Fig. 1 (left). The ridge-like structure is clearly visible, extending to at least 4 units in $\Delta\eta$ as previously observed in Ref. [3]. However, at higher $5 < p_T^{trig} < 6$ GeV/c as also presented in Fig. 1 (right), the near-side ridge almost disappears. The jet peak around $(\Delta\eta \approx 0, \Delta\phi \approx 0)$ is truncated for better evidentiating the ridge. The long structure around $\Delta\phi \approx \pi$ extending over all the $\Delta\eta$ interval of the plots corresponds to the back-to-back jet correlations.

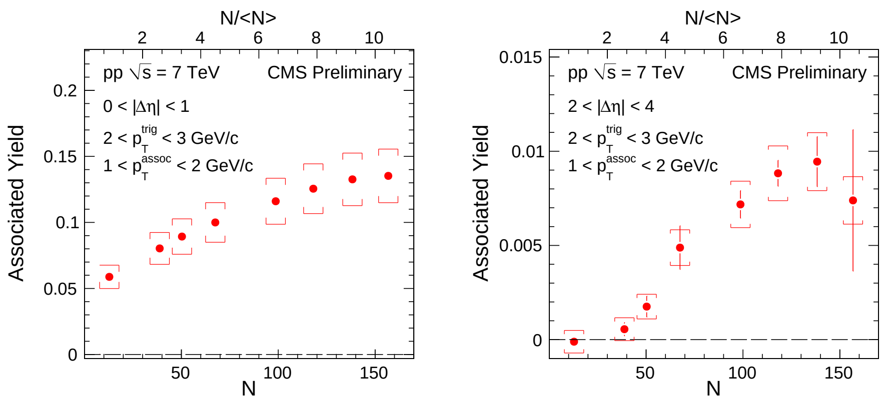


**Figure 2:** Integrated near-side (small $\Delta\phi$ region) associated yield for both the jet, $0.0 < |\Delta\eta| < 1.0$ (left), and ridge, $2.0 < |\Delta\eta| < 4.0$ (right), regions above the minimum level found by the *ZYAM* procedure, as a function of event multiplicity from pp collisions at $\sqrt{s} = 7$ TeV [6]. The bars represent statistical uncertainties, while the brackets correspond to systematic uncertainties.

The discussion in this proceedings focus on the near-side $(\Delta\phi \approx 0)$ ridge structure. For better exploring the detailed properties of both the short-range and the long-range correlations, the 1D $|\Delta\phi|$ azimuthal correlation functions are calculated by integrating over $0.0 < |\Delta\eta| < 1.0$ and $2.0 < |\Delta\eta| < 4.0$, defined as the jet region and ridge region, respectively. The full dependence of the correlations on both $p_T^{trig}$ and $p_T^{assoc}$ is examined in Ref. [6] for $N \geq 110$, in six bins of both $p_T$

variables (36 combinations for each $\Delta\eta$ interval in the jet and in ridge regions).

Next, the near-side (small $\Delta\phi$ region) integrated associated yield is calculated for both jet and ridge regions relative to the minimum of the distribution, i.e., for $|\Delta\phi| < \Delta\phi_{ZYAM}$, where the details of this *zero-yield-at-minimum* (*ZYAM*) procedure can be found in Ref. [4]. Such yields, with $1 < p_T^{assoc} < 2$ GeV/c, are studied as a function of $p_T^{trig}$ for five multiplicity bins ($2 \leq N < 35$, $35 \leq N < 90$, $N \geq 90$, $N \geq 110$, $N \geq 130$) of pp collisions at $\sqrt{s} = 7$ TeV. The jet yield is shown in Ref. [6] to increase with both event multiplicity and $p_T^{trig}$, which was expected due to the increasing contributions from high $p_T$ jets. Differently, the ridge yield is shown in [6] to be almost zero for the first two above mentioned low multiplicity intervals. In the high multiplicity region ($N \geq 90$), the ridge yield first increases linearly with $p_T^{trig}$, reaches a maximum around $p_T^{trig} \sim 2-3$ GeV/c and drops at higher $p_T^{trig}$.

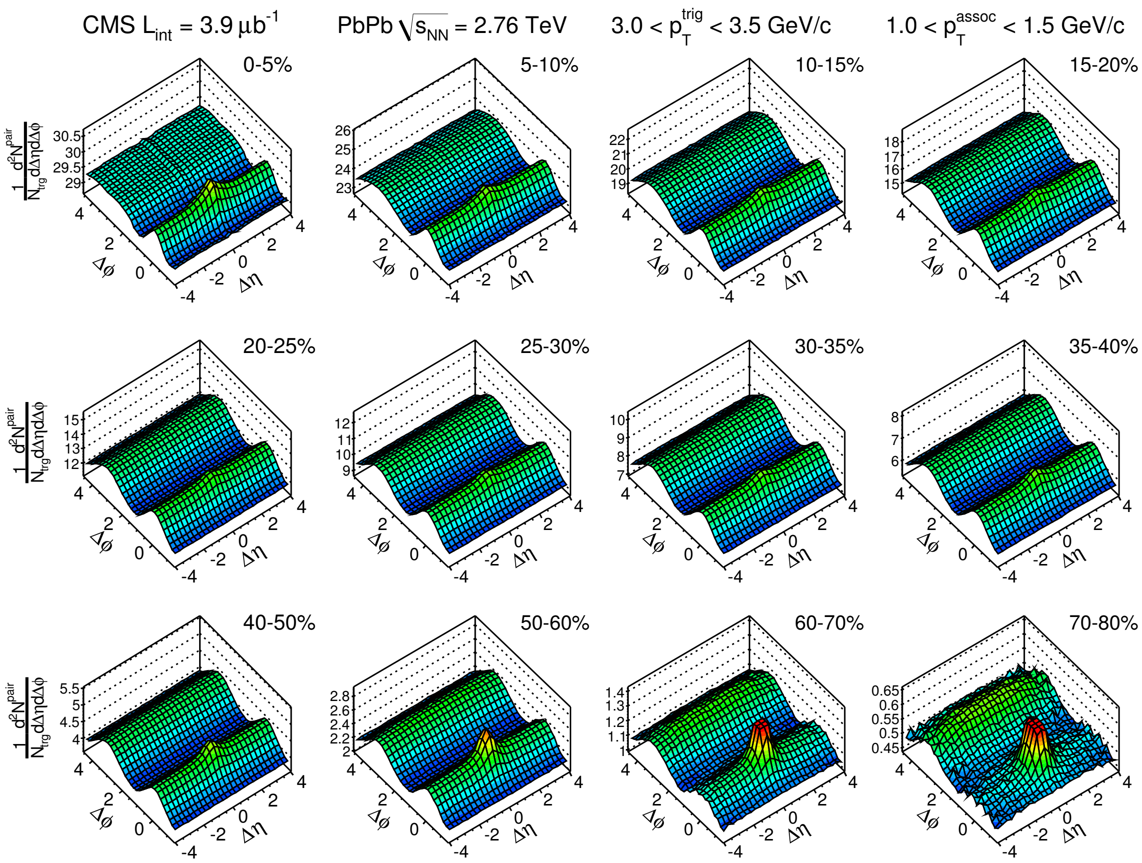


**Figure 3:** 2D per-trigger-particle associated yield of charged hadrons as a function of $\Delta\eta$ and $\Delta\phi$, with $3 < p_T^{trig} < 3.5$ GeV/c and $1 < p_T^{assoc} < 1.5$ GeV/c, for twelve centrality bins of PbPb collisions at $\sqrt{s} = 2.76$ TeV [7]. The peak is truncated in the two most peripheral distributions to evidence the structure around it.

The dependence of the near-side associated yield on multiplicity in the jet and ridge regions is illustrated in Fig.2 for $2 < p_T^{trig} < 3$ GeV/c and $1 < p_T^{assoc} < 2$ GeV/c, corresponding to the $p_T$ bins where the ridge effect appears to be strongest. As seen in Fig. 2, the effect gradually turns on for event multiplicities around $N \approx 50-60$ (about four times the average multiplicity corresponding to minimum bias pp events, $< N_{min\ bias} >\approx 15$) and continuously increase, although with current statistical and systematic uncertainties it is not conclusive if it saturates when reaching $N \approx 120$.

The dihadron correlation measurements in PbPb collision have been systematically performed as a function of transverse momentum and centrality. The average number of participant nucleons $< N_{part} >$ can be calculated for each centrality bin using the Glauber Monte Carlo model [9]. As an example, in Ref. [6] the dihadron correlations in $(\Delta\eta, \Delta\phi)$ are shown for different centralities, displaying also the corresponding $< N_{part} >$ in each panel, with $4 < p_T^{trig} < 6$ GeV/c and with $2 < p_T^{assoc} < 4$ GeV/c. As another illustration, the centrality dependence of the 2D dihadron correlations in PbPb collisions is shown in Fig. 3 for trigger particles with $3 < p_T^{trig} < 3.5$ GeV/c and associated particles with $1 < p_T^{assoc} < 1.5$ GeV/c [7]. This analysis is based on a data sample of PbPb collisions corresponding to an integrated luminosity of approximately $3.9\mu b^{-1}$. The top left corner corresponds to the 0-5% most central collisions. Progressively, the results for 70-80% centrality are reached in the bottom right corner, which corresponds to the most peripheral collisions analyzed. In the most central PbPb collisions, a clear and significant ridge-like structure is observed at $\Delta\phi \approx 0$, which extends all the way to the limit of the measurement, corresponding to $\Delta\eta = 4$. For mid-peripheral collisions, a $\cos(2\Delta\phi)$ pattern attributed to elliptic flow becomes evident. In the most peripheral collisions, the near-side ridge structure is largely diminished, although the away-side back-to-back jet correlations can be clearly seen at $\Delta\phi \approx \pi$, largely spread along $\Delta\eta$. A tiny bump at $\Delta\eta \approx 0$ along the entire $\Delta\phi$ range of the correlation function is visible for the two most central bins, an effect due to low-$p_T$ *looping tracks* that pass through the silicon tracker multiple times mainly at mid-rapidity, causing duplicate tracks at the same rapidity but with different azimuthal angles. This effect, however, is negligible compared to the systematic uncertainties in this measurement [7].

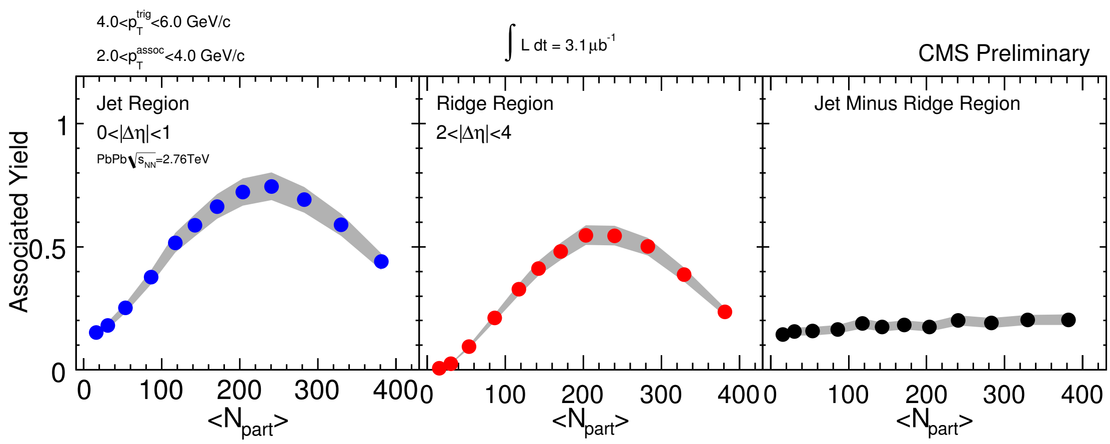


**Figure 4:** Integrated near-side associated yields for $4 < p_T^{trig} < 6$ GeV/c and associated particles with $2 < p_T^{assoc} < 4$ GeV/c above the minimum level found by the *ZYAM* procedure, for the $0 < |\Delta\eta| < 1$ jet region (left), for the $2 < |\Delta\eta| < 4$ ridge region (middle), and for the difference jet–ridge region (right), as a function of $< N_{part} >$, for PbPb collisions at $\sqrt{s_{NN}} = 2.76$ TeV [6]. No flow is subtracted in any of the cases. The gray bands correspond to the total systematic uncertainties as determined in Ref. [4].

As done in Ref. [4], to quantitatively examine the features of short-range and long-range azimuthal correlations, 1D $\Delta\phi$ correlation functions are calculated by averaging the 2D distributions in the jet ($0 < |\Delta\eta| < 1$) and ridge ($2 < |\Delta\eta| < 4$) regions, respectively. In Ref. [6], the per-trigger-particle associated yields of charged hadrons as a function of $\Delta\phi$ is analyzed for $4 < p_T^{trig} < 6$ GeV/c and associated particles with $2 < p_T^{assoc} < 4$ GeV/c, for twelve centrality ranges of PbPb collisions at $\sqrt{s} = 2.76$ TeV. The *ZYAM* methodology is then applied to the $\Delta\phi$ distributions, without any flow subtraction, similarly to what is discussed above in the case of high multiplicity pp collisions. The corresponding results from Ref. [6] are shown in Fig. 4. A strong centrality dependence is observed in the associated yields coming primarily from the long-range ridge region. By subtracting off the ridge region yield from the jet region yield, the residual jet region associated yield is found to be largely independent of centrality, a feature of the data similar to that seen at RHIC energies.

The experimental observations discussed above raise some interesting points for reflection. First, the finding of the long ridge structure in dihadron correlations in high multiplicity events in pp collisions at 7 TeV, only seen before in high energy heavy ion collisions, is striking in itself, perhaps suggesting that protons could behave similarly to small nuclei in such conditions. Besides, other very interesting similarities can be established between such results and those from PbPb collisions at 2.76 TeV. In particular, examining the near-side per-trigger integrated associated yield shown in Figures 2 and 4, a resembling characteristic is observed regarding the onset of the ridge structure. The plot on the right of Fig. 2 suggests that the ridge-like behavior starts to manifest itself for $N/ < N_{min\,bias} > \approx 3-4$, i.e., for events with multiplicity $\approx 50-60$. From Fig.4, it can be seen a similar connection with increasing centralities in PbPb collisions, suggesting an onset at $< N_{part} > \approx 40-60$, corresponding to mid-peripheral events. These facts may pose challenges to theoretical models to simultaneously explain such different systems and their similarities at once.

## References


[1] PHENIX Collaboration, *Dihadron azimuthal correlations in Au+Au collisions at* $\sqrt{s_{NN}} = 200$ *GeV*, *Phys. Rev.* **C78** (2008) 014901 [nucl-ex/0801.4545].

[2] STAR Collaboration, *Long range rapidity correlations and jet production in high energy nuclear collisions*, *Phys. Rev.* **C80** (2009) 064912 [nucl-ex/0909.0191].

[3] CMS Collaboration, *Observation of long-range, near-side angular correlations in proton-proton collisions at the LHC*, *JHEP 09* (2010) 091 [nucl-ex/1009.4122].

[4] CMS Collaboration, *Long-range and short-range dihadron angular correlations in central Pb Pb collisions at* $\sqrt{s_{NN}} = 2.76$ *TeV*, *JHEP 07* (2011) 076 [nucl-ex/1105.2438].

[5] ALICE Collaboration, *Harmonic decomposition of two-particle angular correlations in PbĐPb collisions at* $\sqrt{s_{NN}} = 2.76$ *TeV*, (2011) arXiv: nucl-ex/1109.2501.

[6] CMS Collaboration, *Centrality and multiplicity dependence of dihadron correlations in PbPb and pp collisions*, (2011) *CMS PAS HIN-11-006*.

[7] CMS Collaboration, *Centrality dependence of dihadron correlations and azimuthal anisotropy harmonics in PbPb collisions at* $\sqrt{s_{NN}} = 2.76$ *TeV*, (2012) arXiv: 1201.3158.

[8] CMS Collaboration, *The CMS experiment at the CERN LHC*, *JINST* **0803** (2008) S08004.

[9] B. Alver, M. Baker, C. Loizides, P. Steinberg, *The PHOBOS Glauber Monte Carlo*, (2008) arXiv: 0805.4411.